Acta Scientiarum

http://periodicos.uem.br/ojs
ISSN on-line: 1807-8664
Doi: 10.4025/actascitechnol.v46i1.66835

Effect of Land Use/Land Cover Maps on CN Method: Case Study over Kahramanmaras

Arif Oz and Muhammet Omer Dis*

Department of Civil Engineering, Faculty of Engineering and Architecture, Kahramanmaras Sutcu Imam University, 46050, Onikisubat, Kahramanmaras, Turkiye. *Author for correspondence. E-mail: momerdis@ksu.edu.tr

ABSTRACT. The impact of Land Use/Land Cover (LULC) data obtained from various spatial resolution satellites on the distribution of the Curve Number (CN) across Kahramanmaras using the Soil Conservation Service (SCS)-CN technique was investigated in this research. This study aimed to examine the effect of LULC on runoff due to increasing urbanization in the last century and the conversion of forest areas to agricultural lands. CORINE data with a spatial resolution of 100 m, and Sentinel-2A data with spatial resolutions of 10, 20, and 60 m were utilized in the analysis. The results reveal that only the average CNs of the products are in close proximity, while there are significant discrepancies in the CN variation over the maps as the spatial resolution increases. The Sentinel-2A satellite findings revealed higher CN values compared to the CORINE dataset over the study area where three geographical regions, namely the Mediterranean, Eastern Anatolia, and Southeastern Anatolia. Additionally, the results show that an increase in urbanization triggers surface runoff potential and reduces it in agricultural and forest areas in the city. Thus, the updated and higher spatial resolution of LULC promises accurate flood forecasting and/or more scientific potential drought estimation as well as other hydrological applications.

Keywords: CN; GIS; LULC; remote sensing; rainfall-runoff.

Received on January 26, 2023.
Accepted on February 05, 2024.

Introduction

Water is of vital importance because it has been defined as the source of life throughout human history. Mankind, therefore, has endeavored to use water resources effectively and maintain their needs at an adequate level. As a result of global warming, which has made its impact more felt throughout the world in recent years, a significant increase in temperatures has been observed, while a decreasing trend in precipitation has become an indisputable fact. In addition, with increasing population and industrial activities, irregular urbanization, and reduction of forest areas, serious declines in groundwater levels occur. According to the report of the Intergovernmental Panel on Climate Change (IPCC) in 2013, the average surface temperature has increased by 0.89 °C based on in-situ measurement records from 1901 to the present. The global surface temperature is still in the direction of rising trends, and the current glaciers on Earth are disappearing at approximately 275 million tons per year. The amount of sea-level rise on a global scale has reached 19 cm since 1901. At the same time, this increase is 3.2 mm annually. In extreme weather, many changes have occurred since 1950, such as increases in the frequency of heat waves and heavy rains in certain regions (Solomon et al., 2013).

However, from the past to the present, water has been in a continuous hydrological cycle on the Earth. The water, rising to the atmosphere by evapotranspiration from the oceans and earth, falls back to the surface in the form of precipitation from the atmosphere. The water falling into the soil generates groundwater with infiltration while excess water remaining from seepage reaches the rivers and oceans with the surface flow. The rainfall-driven runoff estimation plays an important role in hydraulic structure designs and the design of water resources projects. Rainfall-runoff simulations lead to the construction and design of the many hydrological buildings interacting with rivers and lakes (i.e. roads, bridges, dams, culverts, etc.). In addition, precipitation-based models are crucial for long-term water management and pumping stations (Nickman, Lyon, Jansson & Olofsson, 2016; Júnior, Stosic, Stosic, Jale & Xavier, 2018; Jehanzaib, Ajmal, Achite & Kim, 2022; Zhu, Wei, Zhang, Xu & Qin, 2023). For rainfall-runoff modeling, it is possible to make an easy decision in the face of a problem or analysis and to evaluate the data together by overlapping the data in layers via

Geographic Information Systems (Geographic Information Systems [GIS]. 2021) applications with today's evolving technology. In addition, there is an opportunity to recognize, process, modify, and interpret almost all data at once. The river drainage network in a watershed and basin morphology can be determined, and a catchment can be delineated and divided into sub-basins using GIS applications (Meric, 2004; Strager et al. 2010; Ray, 2018).

Various hydrometeorological modules can be used to process the geomorphometric structure of a region and the physical characteristics of the basin into hydrological models. Depending on the purpose of the application objectives, access to the dataset and the morphological structure of the region, SWAT (Soil and Water Assessment Tool), MIKE SHE (Système Hydrologique Européen), HEC-HMS (Hydrologic Engineering Center- the Hydrologic Modeling System), HEC-RAS (River Analysis System), CREST (the Coupled Routing and Excess Storage), WMS (the Watershed Modeling System) and so on can be applied (Abbott, Bathurst, Cunge, O'Connell & Rasmussen, 1986; Gassman, Reyes, Green & Arnold, 2007; Scharffenberg, & Fleming, 2010; Daniel et al. 2011; Wang et al. 2011; Beven, 2012; Enemark, Peeters, Mallants & Batelaan, 2019). One of the most preferred models is HEC-HMS software developed by the U.S. Army Corps of Engineers and this software provides both event-based and continuous hydrological modeling in different-sized basins in different parts of the world. For example, in the study conducted on Yenicegoruce Basin, daily precipitation and temperature data were obtained. The characteristics of the region (i.e., land use, hydrological soil groups, and digital elevation model dataset) were derived in the GIS environment, and basin hydrological modeling was carried out with the help of the HEC-HMS module. Precipitation-based runoff processes were simulated using daily data, and model parameters were calibrated in six years (1997-2002) while they were validated for three years (2003-2005). In the study, it is stated that the rainfall-runoff simulation results are in the acceptable range while the results on the sub-basin basis are left open to improvement (Mesta et al. 2019).

All hydrological models simulate the precipitation-runoff process using mathematical methods. Although many methods are used in rainfall-driven runoff modeling, the Soil Conservation Service-Curve Number method (SCS-CN) is widely applied in hydrometeorological simulations for small catchments around the world (Mishra & Singh, 1999; Das & Paul, 2006; Beven, 2012; Cubuk & Dis, 2022). Geomorphic datasets (i.e., Digital Elevation Model (DEM), Land Use/Land Cover (LULC), and Hydrological Soil Groups (HSG)) are required for the implementation of this method. Currently, it is possible to obtain easy and complementary data for applications using remote sensing methods. Remote sensing images allow thematic acquisition of data on subjects, such as land use, vegetation cover, soil groups, and land topography of the basins. These satellite datasets can be stored in the GIS database after projection adjustments. Then, these data are made available with the necessary modifications, new data entry, and analysis for the study area. Various practices have been carried out on numerous topics such as the methods used in the rainfall-runoff simulations, runoff coefficients estimation, and the contribution of remote sensing methods to these modules. For example, hydraulic and meteorologic observation stations provide number of data while there may not always be a station in every basin. Thus, these necessary data can be tried to be obtained by remote sensing methods. For instance, the rainfall-runoff relationship was investigated by using the SCS-CN method with remote sensing methods in the Havran Watershed (Turkiye). In the study, the LULC data was acquired from the Spot XS satellite with 20 m spatial resolution while the HSG was obtained from the 1:25000 scale soil map. Applying a dataset with approximately 30-year (1975-2003) precipitation measurements as input data in the SCS-CN method, rainfall-driven runoff simulations were acquired with a high correlation for the flow observations (Ozdemir, 2007). In a study conducted in the city of Al-Kadisiye, Iraq, the most suitable regions for water collection and storage were determined using the SCS-CN model and the GIS program. Potential catchment areas were determined using the SCS-CN model as an intermediate input to simulate surface runoff (Al-Khuzaie, Janna & Al-Ansari, 2020). In another study, the rainfall-runoff process was estimated by the HEC-HMS model in the Jianghe Basin (Northern China) which has semi-arid and sub-humid climate characteristics. The applicability and accuracy of different components and modules (such as the Initial Constant-Rate, SCS-CN, Kinematic Wave, SCS unit hydrograph, and Muskingum) in HEC-HMS were investigated, in the region. It has been stated that the SCS-CN model gives more acceptable results, depending on the hydrological characteristics and basin characteristics, when the simulation results are compared with the observed hydrograph values for this climatological region (Jin, Liang, Wang & Tumula, 2015). In the study of the Gaza Strip, the impact of land use change over the years on potential flow volumes was estimated using a simplified GIS-based SCS-CN method (Al-Juaidi, 2018). Since the standard SCS-CN technique is time-consuming, GIS

and HEC-GeoHMS were applied in a holistic sense over the region. More accurate CN and flow volume results supported the applicability of the approach compared to the rational method. Baduna Koçyiğit and Akay (2018) predicted hydrograph values by hydrometeorological analysis over the Akcay Basin (Western Black Sea Region). In the study, it was digitized with the help of Arc-GIS using a 1/25000 scale topographic map, and the region was divided into seven different sub-basins. Hydrological processes were analyzed by using the SCS method in the simulations of infiltration processes, the Clark Unit Hydrograph method in the estimation of effective rainfall-runoff transformations, and the lag time method in flood routing in the stream. To be used in the SCS method, the soil type and land use maps created in 1984 were obtained and the CN values were generated. Then, the effective precipitation for each sub-basin was acquired via these values. In the Clark method, which converts effective precipitation to runoff, the concentration time is determined according to the SCS method. In another example, the hydrometeorological process in the Texas State San Antonio River Basin (USA) was performed using HEC-HMS, and the precipitation-based runoff was predicted by the SCS-CN method. As a result of this study, it can be concluded that it will benefit future modeling studies by providing a tool for hydrological predictions of floods at the regional scale (Knebl, Yang, Hutchison & Maidment, 2005).

Another important issue that should be mentioned in the rainfall-runoff relationship is the change in land use/cover. In recent years, very significant increases have been seen in agricultural activities and urbanization due to the high population growth rate. It can be observed that forest areas are shaped towards agricultural areas and urban sprawl. This situation has led to the differentiation of water interactions, which have a continuous hydrological cycle. The flash flood events that occur in areas with irregular urbanization are the largest examples of this. Many studies on this subject have been conducted by researchers worldwide. For instance, the impact of changes in LULC and urbanization on floods was investigated for the urbanized basin of the Oshiwara River in Mumbai (India). For the study area, LULC evolution was estimated between 1966, 2001, and 2009 using the DEM and satellite images. According to this, the change between 1966-2001 was slower than the change between 2001-2009. As a result of these changes in urbanization, it was determined that the flood risk increased by 22.27% (Zope, Eldho & Jothiprakash, 2016). Rizeei, Pradhan, and Saharkhiz (2018) analyzed the effect of climate and LULC dynamics on runoff variation. For this purpose, study conducted in the Semenyih Basin (Malaysia), various LULC classes attained from the Sot-5 satellite and land transformation model were applied to capture LULC variation during 2000 and 2010 and estimate 2020. In the study, the SCS-CN approach was applied to simulate surface-flow maxima, and it was concluded that urbanization and deforestation resulted increment in runoff until 2010 exceeding in 2020. This important human activity on LULC dataset can cause floods of immense size. Unfortunately, however, the resultant variation in peak discharges and runoff volume scenarios is noticed after a long time. Abdulkareem, Sulaiman, Pradhan, and Jamil (2018) conducted a study in the Kelantan River Basin (Malaysia) to analyze the impact of past and current (1984, 2002, and 2013) LULC changes on runoff volumes. The study showed that change in LULC for time affected peak discharges for different return periods while it is stable at higher return periods (50 years). Per the report issued by the Ministry of Agriculture and Forestry General Directorate of Water Management of the Republic of Turkiye, projections indicate that the frequency and severity of floods will rise as a consequence of human activities and climate change, resulting in increased damage (Su Yönetimi Genel Müdürlüğü [SYGM], 2018).

Kahramanmaras, which is the eleventh city of Turkiye with its surface area and the eighteenth city of Turkiye regarding its population, is located in a combination of three geographical regions, namely the Mediterranean, Eastern Anatolia, and Southeastern Anatolia. Additionally, the city has experienced a great deal of immigration due to the Syrian civil war in recent years. Owing to the importance of the cities in terms of both location and population, updated LULC maps are vital for hydrological applications. For this reason, CN values were obtained by using the SCS method for two different LULC dataset obtained using remote sensing methods via a GIS environment. It also aims to show possible differences in the precipitation-runoff coefficients due to the spatial resolution of the data.

Materials and methods

Kahramanmaras is located Southeastern of Turkiye with an area of 14,346 km² between 37-38 north parallels and 36-37 east meridians. It is covered 61% by mountainous and forested areas, 35% by agricultural areas, and the remaining parts are water bodies and artificial areas. The higher elevation parts of its mountains generally consist of bare rocks while its lower elevations are covered with forest texture. The city

is situated Mediterranean region at the junction of Central Anatolia, Eastern Anatolia, and Southeastern Anatolia. In addition, the city has numerous natural and artificial lakes. The city's geographical location, surface area, elevation gradient, and other factors have resulted in climate characteristics that are more closely aligned with the "Degraded Mediterranean Climate". However, due to the size of the provincial borders, the transition zone between the Mediterranean Climate and the Continental Climate, one of the macro climate types in Turkey, is occasionally encountered in the districts. For example, the Mediterranean climate prevails in the southern regions of the city, whereas the continental climate prevails in the northern regions (Cosun & Karabulut, 2009; Cinar, 2023; Dis, 2023).

The SCS-CN method was developed by the United States Department of Agriculture in 1954 and was published as a handbook (Mishra & Singh, 2003). This approach was used to estimate the excess water after infiltration losses for precipitation-based events. The DEM, LULC, and HSG maps are the most basic input dataset used for the application of this method. For this purpose, DEM data for Kahramanmaras was obtained with a 30x30 m spatial resolution from the United States Geological Survey (USGS) website (GIS, 2021). After the necessary projection and basin delineation, slope variation and elevation variation analyses over the watershed can be performed from this dataset via the Arc-GIS environment. As shown in Figure 1, the catchment has an elevation gradient increasing from south to north and the elevation varies from 142 to 3,067 Mean Sea Level (M.S.L). As can be seen from the elevation map, the city consists of 59.7% mountains.

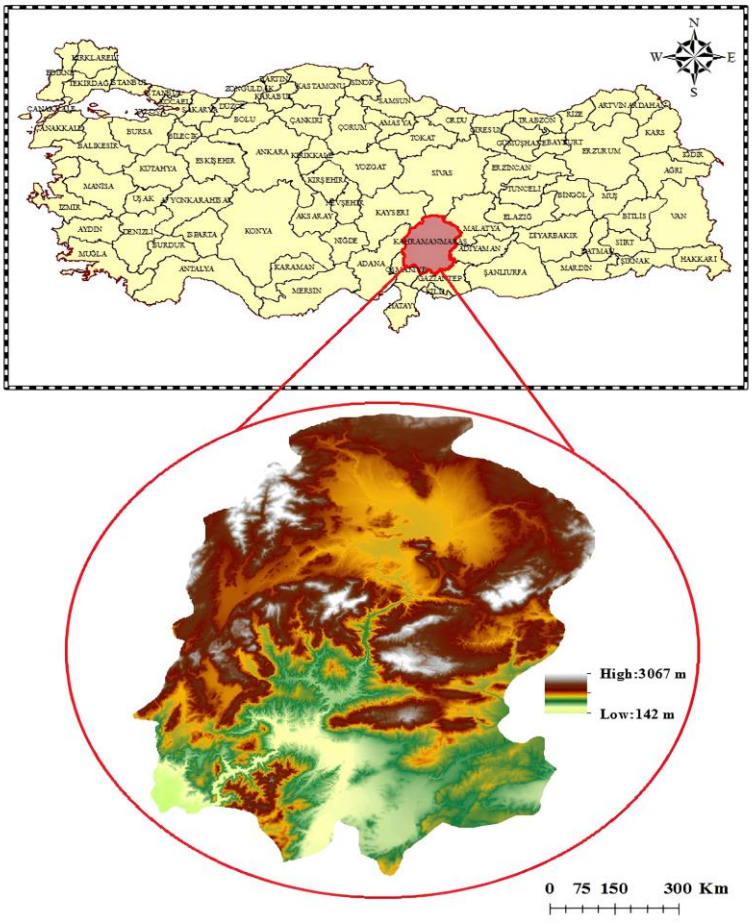

Figure 1. Kahramanmaras Province Digital Elevation Model.

The water balance in Equation 1 can determine the flow in any specific area and time frame (De Ridder & Boonstra, 1994; Cubuk &Dis, 2022). In the equation P symbolizes rainfall depth (mm), I_a denotes initial abstraction (mm), F represents infiltration amount (mm), and Q is runoff depth (mm). According to the SCS-CN methodology, Equation 2 can be written as the ratio of the infiltration potential to the ratio of the potential value of direct runoff (Soil Conservation Service [SCS], 1986). When the sum of the surface runoff amount and infiltration heights in Equation 1 is substituted into Equation 2, Equation 3 for the Q value is derived. As can

be seen from "$I_a = \lambda S$" expression, initial abstraction values vary depending on the potential maximum rainfall amount retained by the soil, S, and the rate constant value, λ. Through studies of many small agricultural watersheds, the initial abstraction ratio can be considered as 0.2 (SCS, 1986; Knebl et al., 2005; Elagca & Dis, 2022). When this expression is substituted into Equation 3, Equation 4 is obtained. According to this method, the relationship between rainfall and the runoff depth can be revised as 5, after the necessary adjustments made in Equation 4. S values used in Equation 5 can be calculated with Equation 6 depending on the curve number. As can be demonstrated from Equation 5, CN values play a critical role in the surface runoff estimations that are occurred excess rain over a study area.

$$P = I_a + F + Q \tag{1}$$

$$\frac{Q}{P-I_a} = \frac{F}{S} \tag{2}$$

$$Q = \frac{(P-I_a)^2}{(P-I_a)+S} \tag{3}$$

$$Q = \frac{(P-0.2S)^2}{(P-I_a)+S} \tag{4}$$

$$Q = \frac{(P-I_a)^2}{P+0.8S} \tag{5}$$

$$S = \frac{25\,400-254CN}{CN} \tag{6}$$

Additionally, soil properties were obtained from the European Soil Data Centre (European Soil Data Centre [ESDAC]) database with a spatial resolution of 250 m to create an HSG map for the study area (ESDAC, 2021). Then, the dataset was divided into hydrological soil groups such as A, B, C, and D within the scope of the SCS-CN Method with the help of the Arc-GIS program (Figure 2a). Group A has low flow potential and high infiltration capacity, while Group D, on the contrary, represents soil groups with high runoff potential and low drainage capacity (Mockus et al., 2009). The main soil types over the region were brown soils (25.3%), non-calcareous brown forest soils (20.4%), and brown forest soils (17.22%). Brown soils generally have a medium permeability and runoff potential. As can be seen from Figure 2a, HSG-Group C is composed of a large part of Kahramanmaras Province. It can be considered that Kahramanmaras has low drainage and high runoff capacity for this soil group due to its high slope geographical structure (Elagca & Dis, 2022).

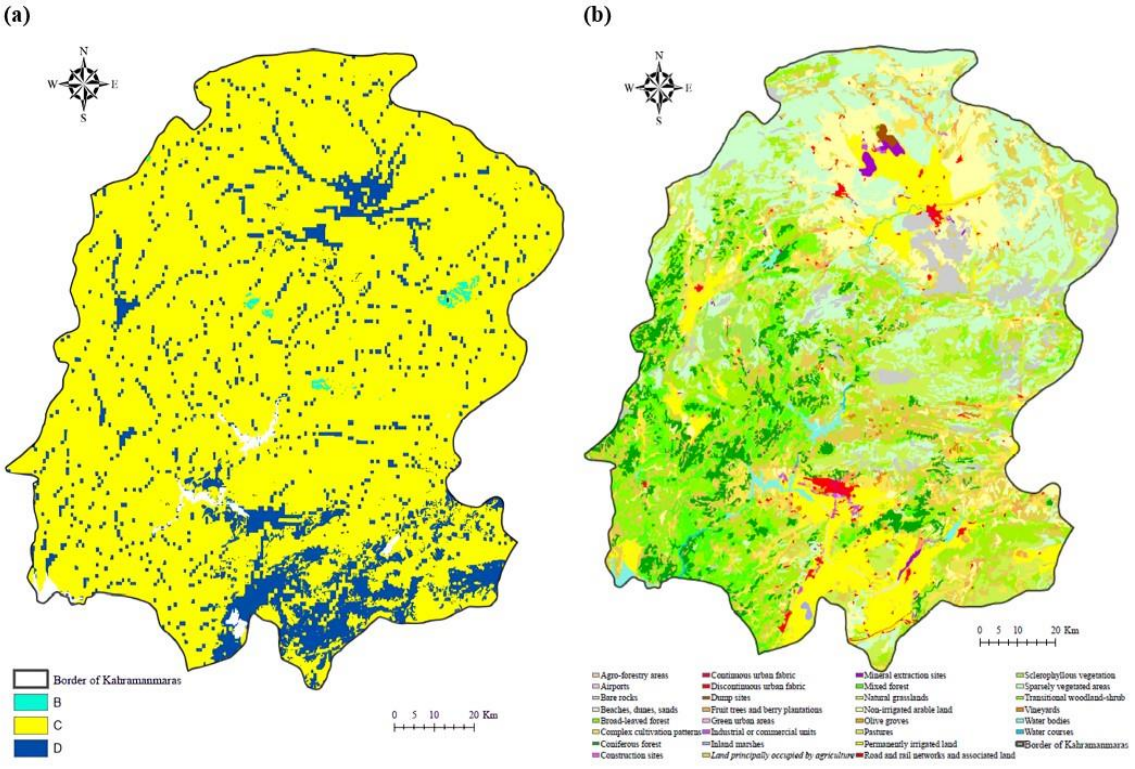

Figure 2. Kahramanmaras Province Hydrologic Soil Group and Land Use/Land Cover Map.

Changes in water supply and quality caused by land use change are becoming a critical issue affecting the hydrological functions of both surface and groundwater (Fohrer, Haverkamp & Frede, 2005; Stonestorm, Scanlon & Zhang, 2009). Therefore, LULC maps are vital importance in determining the flow potential and infiltration capacity over a study area. In this study, LULC data was attained from the CORINE 2018 land cover with 100 m of spatial resolution data (Coordination of Information on the Environment [CORINE], 2021). The CORINE 2018 dataset was derived from satellite images of the Copernicus Land Monitoring Service. The CORINE project was initiated in 1985 to collect information from the European Union on priority environmental issues (i.e., air, water, soil, land cover, and coastal erosion). The acquisition of CORINE maps has typically involved converting images to vector format through satellite photo interpretation at a scale of 1:100,000. In recent years, a growing number of nations have acquired CORINE by generalizing their national LULC datasets to finer scales (Alvarez & Olmedo, 2023). As can be seen from the CORINE LULC map, the city consists mainly of forest areas and rocks, whereas the density of agricultural areas should not be ignored (Figure 2b). In this study, the LULC classification was conducted based on the Republic of Turkiye Ministry of Agriculture and Forestry CORINE portal, and the classification is given in Table 1 (Republic of Türkiye Ministry of Agriculture and Forestry [MAF], 2021).

Table 1. CORINE 2018 Kahramanmaras LULC classification.

No	Layer	Area (ha)	Percentage (%)
1	Sparse Plant Areas	268,957.86	18.52
2	Plant Exchange Areas	186,860.2	12.87
3	Natural Grasslands	180,511.84	12.43
4	Mixed Agricultural Fields	163,005.58	11.22
5	Irrigated Arable Lands	174,562.58	12.02
6	Continuously Irrigated Areas	155,158.31	10.69
7	Mixed Forests	202,650.55	13.95
8	Bare Cliff	54,268.17	3.74
9	Pasture Fields	14,056.45	0.97
10	Water Bodies	13,930.41	0.96
11	Non-Continuous Settlements	6,252.98	0.43
12	Fruit Fields	10,221.81	0.70
13	Discontinued Rural Settlements	5,727.37	0.39
14	Mineral Extraction Sites	9,443.62	0.65
15	Beaches, Sands	2,382.19	0.16
16	Waterways	1,643.71	0.11
17	Continuous City Structure	1,711.41	0.12
18	Marshes	828.03	0.06

As shown in Figure 2b and Table 1, numerous groupings are available for the CORINE LULC data. Therefore, this classification can be regrouped under four main headings to prevent confusion and provide convenience in interpreting the study area, as shown in Table 2.

Table 2. Kahramanmaras reclassified LULC.

No	Layer	Area (ha)	Percentage (%)
1	Artificial Areas	23,135.37	1.59
2	Agricultural Areas	517,004.74	35.60
3	Forest and Semi-Natural Areas	895,630.81	61.68
4	Water Bodies	16,402.15	1.13

Additionally, in this study, the Sentinel-2A satellite dataset, which can provide higher resolution LULC maps and allow a chance to compare with CORINE in terms of accuracy, was used. The dataset can be complementarily accessible from this satellite sent into orbit by the European Space Agency (European Space Agency [ESA]) (ESA, 2015). The Global Monitoring for Environment and Security (GMES) Sentinel-2 mission is designed to provide long-term continuity for services that depend on high-resolution, multi-spectral optical observations of terrestrial surfaces across the globe. Sentinel-2 actively supports terrain monitoring, emergency response, and security services. Contrary to CORINE 2018, it provides users with 10, 20, and 60 m spatial resolution data. Satellite images with zero cloudiness were obtained from the Sentinel-2A satellite for the date of December 2020. However, land use/cover information requires to be derived with Arc-GIS

environment although Sentinel-2A satellite provides high-quality spatial resolution dataset to users. Numerous statistical prediction methods are available for developing this information. Among these approaches, the method that best estimates the parameters of a model in statistics is Maximum Likelihood Estimation (MLE). MLE is an estimation method that selects the parameters for which the observations made in this approach are most likely within the statistical model used. The maximum likelihood estimator for the evaluation parameter based on the assumed distribution of random variable X is shown in Equation 7.

$$L = (\theta; x_1, x_2, \ldots\ldots, x_n) = \prod_{i=1}^{n} f_x(x_i; \theta) \quad (7)$$

In this, it is more convenient to maximize the logarithmic probability than Θ. For the exponential distribution, when "$\log L(\theta) = n \log(\theta) - \sum_{i=1}^{n} \theta x_i$" expression equals to zero, the parameter estimator is obtained as "$\widehat{\theta} = \frac{1}{\bar{x}_n}$". However, these methods can be easily calculated with the help of many computer applications. In the Arc-GIS environment, a substantial number of samples were chosen from the raster data set obtained from the Sentinel-2 satellite for each classification group. Then, the program utilized the MLE method to classify the entire region. Therefore, a more reliable LULC map was modeled by selecting samples for each classification group using the MLE method on the Arc-GIS module.

After the aforementioned dataset was attained and analyzed, LULC and HSG maps were combined in the Arc-GIS environment to derive the CN maps. The CN look-up table can be used to determine the CN values over the study area (Table 3). These values vary with different soil groups and land use patterns. For instance, HSG-Group A represents low runoff potential with high infiltration capacity when fully wetted and mainly composed of sand and gravel with high permeability and well-to-extreme drainage. The HSG-Group B has medium and good drainage rates when fully wetted. Group C, on the other hand, is soils with a medium- and fine-textured solid that prevents the flow with a slow conduction velocity when they are completely wet. Finally, HSG-Group D is almost impermeable soil with high runoff potential and very slow conduction velocity when fully wetted. It can consist of clay with swelling potential soils and/or over shallow groundwater (Dizdar, 1984). The CN values were obtained based on various HSG and LULC types using the SCS National Engineering Handbook-Section 4 guide (SCS, 1986). Then, CN values were determined using the Hydrologic Engineering Center's Hydraulic Modeling System-Geospatial Hydrology module (Hec-GeoHMS) utilizing these data.

Table 3. CN look up table (Chadli, Kirat, Laadoua, & El-Harchaoui, 2016).

Land Use Value	Description	Hydrological Soil Groups			
		A	B	C	D
1	Artificial Areas	57	72	81	86
2	Agricultural Areas	67	77	83	87
3	Forest and Semi-Natural Areas	30	55	70	77
4	Water Bodies	100	100	100	100

Results and discussion

Slope values are important for determining the flow direction over a region. Thus, a slope map was also obtained from the DEM data using Arc-GIS, and most of these values were above 60% (Figure 3).

Since there was too much classification in the CORINE 2018 LULC map on the Arc-GIS program, the map was rearranged under four main headings, as shown in Figure 4a. This regrouping was performed to facilitate the interpretation of the LULC over the region. The map created by selecting samples for each classification group using the MLE approach of land use dataset obtained from the Sentinel-2A satellite with high spatial resolution is shown in Figure 4b. Thus, it is possible to compare the LULC maps of the two satellites with different spatial resolutions.

First, in the two LULC maps obtained, the water surfaces in the region were similarly captured. As can be seen from Figure 4a, in the LULC maps of the region obtained using CORINE 2018, it is observed that artificial areas have a lower percentage, while agricultural areas are denser. On the other hand, in Figure 4b, the eastern and northern regions appear to be artificial areas obtained using Sentinel-2A since this product is more updated and has a higher resolution than CORINE 2018. In addition to the spatial resolution effect, the increasing population in agricultural areas in recent years and the increasing construction and industrial studies due to this population growth can attributed to this.

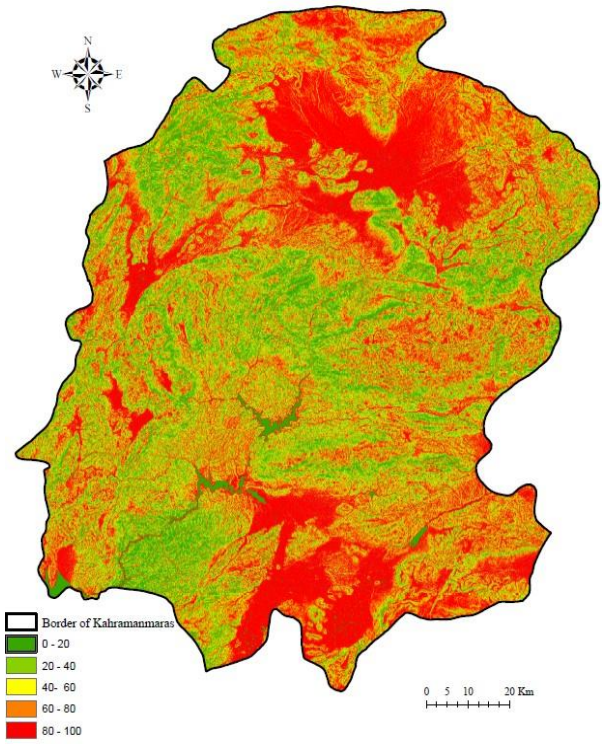

Figure 3. Kahramanmaras Province Slope Map.

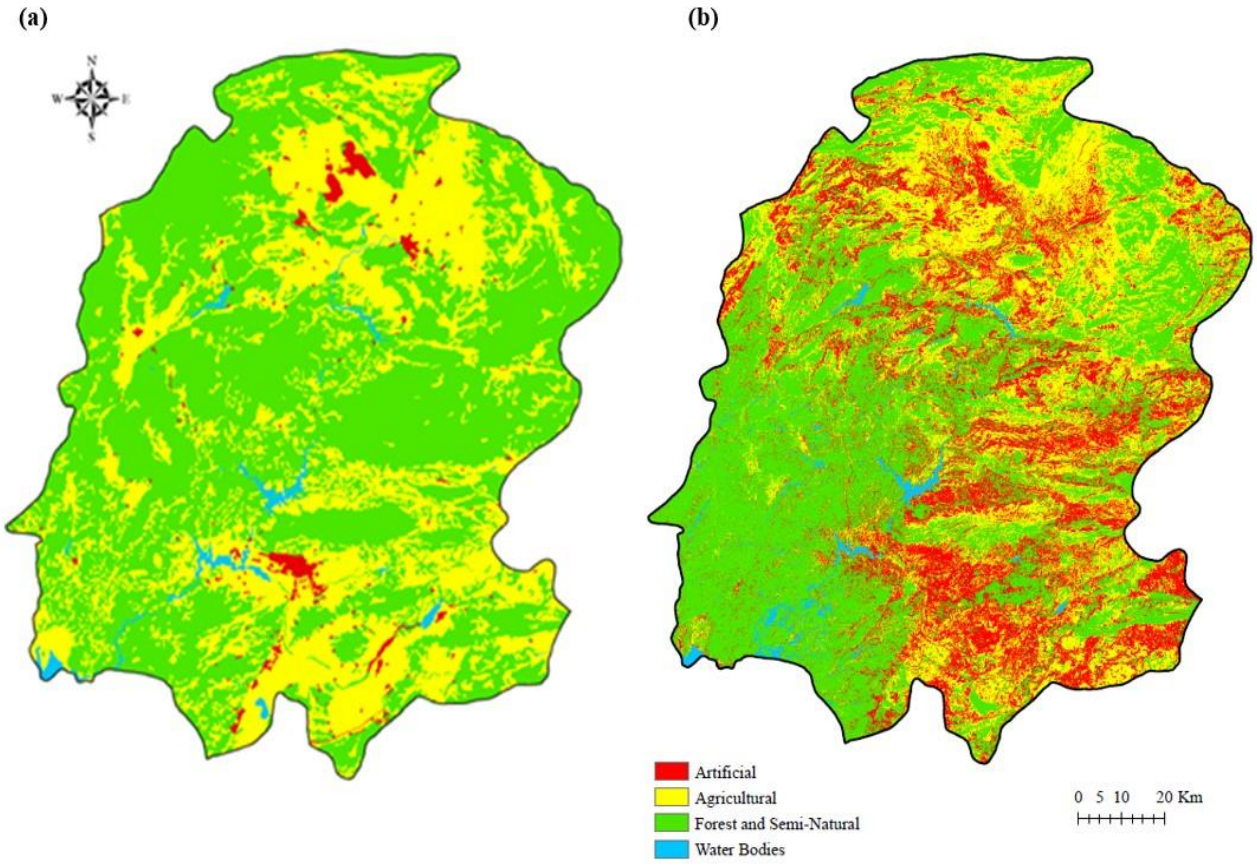

Figure 4. a. Re-classified CORINE 2018 LULC map; **b**. Sentinel-2A LULC map.

CN values were calculated by combining the DEM and HSG maps with two different LULC products using the HEC-GeoHMS module. As a result of the analysis, the distribution maps of two different CN variations shown in Figures 5a and 5b by applying CORINE 2018 and Sentinel-2A satellite dataset, respectively. In the CNs obtained from the CORINE 2018 LULC data, it was observed that the majority were in two ranges (55-70

and 80-90). Values of 55-70 are generally seen in areas representing forested and agricultural areas whereas the CN values of 80-90 are in regions with artificial areas and high slope landforms.

However, as a result of the CN calculations obtained from Sentinel-2A LULC data, it was observed that the majority of them were between 80-90 and affected larger areas. The reason for these high flow rates is due to the fact that the Sentinel-2A satellite provides up-to-date LULC data. As a result of population growth and increasing irregular urbanization and industrialization, infiltration of excess surface runoff has become more problematic. In addition, values of 55-70 are mostly observed in the western part of the city and this value range is smaller than that of the CORINE map.

These results show that the LULC map is an important data input for obtaining CNs; consequently, these numbers have a significant effect on rainfall-runoff mechanisms. For example, high CN values represent low drainage capacity, resulting in a high amount of runoff. For this reason, it can be said that the risk of flooding with high CNs may cause serious dangers over the region. When these two maps were considered together, the presence of forested areas as land cover in the western part of Kahramanmaras generally produced lower CNs results. In addition, the effect of the spatial resolution on the results should not be ignored.

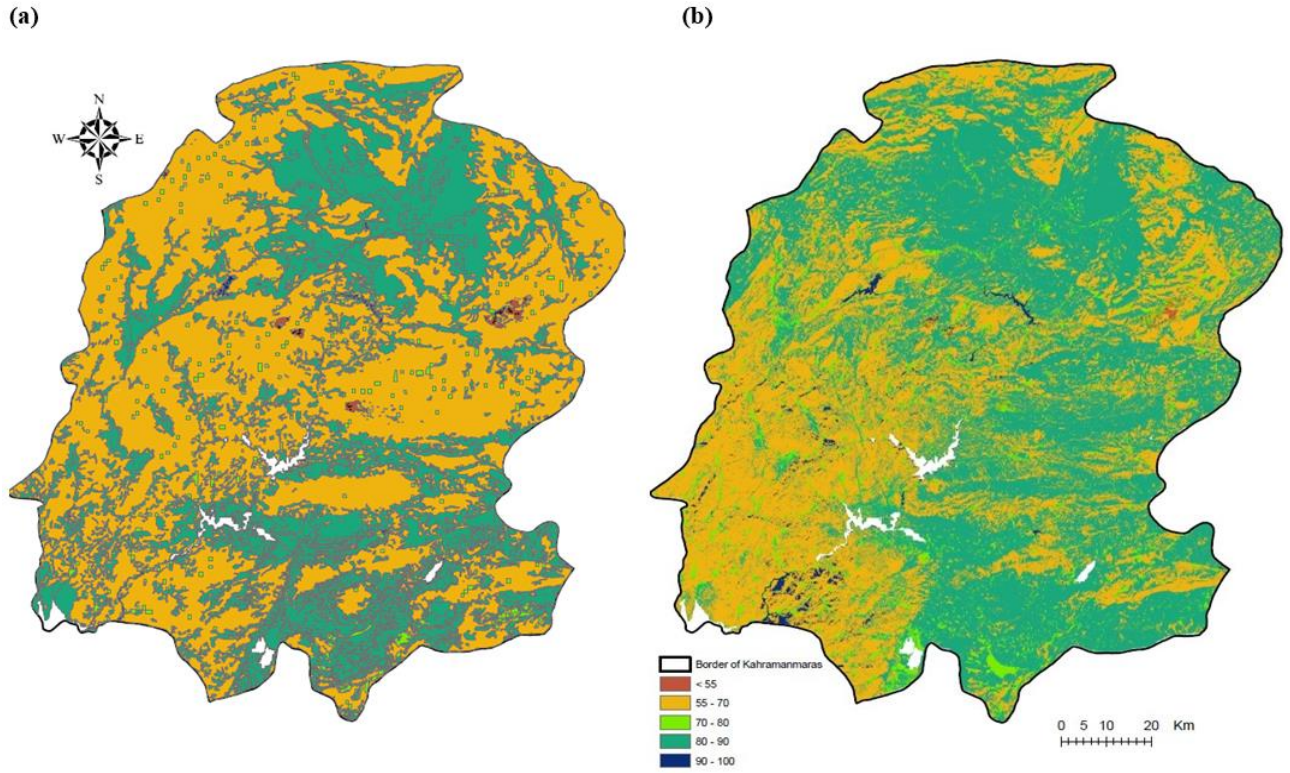

Figure 5. a. CN distribution based on CORINE 2018; **b.** CN distribution based on Sentinel-2A.

The management of water resources is crucial for sustainable development in regions. Water supply and protection from excess water rely on an effective hydrological analysis of the morphological and environmental aspects of a watershed. To obtain accurate results from runoff simulations, it is essential to establish a precise basin definition. This study revealed that rainfall-driven runoff estimates depend on CN values, which vary especially based on the LULC dataset. Elagca & Dis (2022) obtained CN values between 67.93 to 79.84 utilizing the CORINE 2018 dataset in the Ballikaya Basin in southeastern Turkiye. Similar to the results obtained, it was emphasized that the most important parameter in hydrological predictions was the CN parameter which is related to the LULC dataset. Additionally, the results support the findings of Onchevski & Mihara (2021) regarding the SCS-CN method over the Ovche Pole region in Macedonia. They estimated runoff coefficients utilizing the combined CORINE 2018 and Sentinel-2 datasets to use water more efficiently in agricultural activities. They stated that the development of a more precise and detailed land-cover map is of significant importance in hydrological predictions. Phiri et al., (2020), support the findings in this study, claiming that the Sentinel-2 dataset produces high accuracies with classifiers such as MLE analysis and the free access policy increases its use for providing LULC map. By incorporating climatological datasets

(i.e., temperature, evapotranspiration, and precipitation) into the findings of the study, it is possible to develop hydrological applications, such as flood frequency analyses, early warning systems, and etc. for the region. Thus, the integration of the SCS-CN method with GIS will facilitate the efficient utilization of surface rainfall-runoff simulations for basin management purposes.

Conclusion

The primary objective of this research is to determine the rainfall-runoff coefficients within the GIS environment by employing the SCS-CN methodology, in conjunction with data collected from multiple satellites within the boundaries of Kahramanmaras Province. For this purpose, possible differences in the obtained CN values for these satellites and their variations over the region are presented due to their spatial resolution and product effects. Kahramanmaras Province holds a unique position as it lies at the confluence of three geographical regions, namely the Mediterranean, Eastern Anatolia, and Southeastern Anatolia Regions, which are closest to each other in this part of the country. As a result of the analysis, the Sentinel-2A satellite derived higher CN values compared to the CORINE dataset across the region. It may be inferred that the discrepancies in the maps for CN distribution derived from the two-satellite data are attributable to the varying spatial resolution values of the respective satellites. In addition, the fact that the date for obtaining the LULC map with Sentinel-2A satellite is more recent than with the CORINE 2018 product can be shown among the reasons for the higher CN values. The increment in urbanization causes a reduction in forest areas and this highly affects surface runoff.

As evident from the results obtained from the two-satellite data, high CN values occur in areas with urbanization. Therefore, the expansion of urban areas in an unpredictable manner, coupled with the decrease in the extent of forested regions, leads to an increase in surface water runoff, which in turn results in the emergence of flood-related risks. In addition, the destruction of agricultural and forest areas and the irregular and unplanned construction of buildings, roads, and industrial facilities will cause serious damage in case of a possible flood. At this point, LULC maps must be high-resolution and updated for the estimation of rainfall-driven runoff simulations. In case of heavy precipitation that may occur in areas with high levels of urbanization, effective infrastructure and drainage systems should be carried out and the water should be evacuated in a way that does not result destruction. The study highlights the process of comparing the MLE classifiers technique for Sentinel-2A datasets and the CORINE 2018 dataset to enhance the accuracy of LULC maps and obtain CN values utilizing the SCS-CN methodology. This information can be used by policymakers to make more informed decisions and gather essential data for adjusting policies.

References

Abbott, M. B., Bathurst, J. C., Cunge, J. A., O'Connell, P. E. & Rasmussen, J. (1986). An introduction to the European Hydrological System-Systeme Hydrologique Europeen, "SHE", 1: History and philosophy of a physically-based, distributed modelling system. *Journal of Hydrology,* 87(1), 45–59. DOI: https://doi.org/10.1016/0022-1694(86)90114-9

Abdulkareem, J. H., Sulaiman, W. N. A., Pradhan, B. & Jamil, N. R. (2018). Relationship between design floods and land use land cover (LULC) changes in a tropical complex catchment. *Arabian Journal of Geosciences, 11*, 376. DOI: https://doi.org/10.1007/s12517-018-3702-4

Al-Juaidi & A. E. M. (2018). A simplified GIS-based SCS-CN method for the assessment of land-use change on runoff. *Arabian Journal of Geosciences, 11*, 269. DOI: https://doi.org/10.1007/s12517-018-3621-4

Al-Khuzaie, M. M., Janna, H. & Al-Ansari, N. (2020). Assessment model of water harvesting and storage location using GIS and remote sensing in Al-Qadisiyah, Iraq. *Arabian Journal of Geosciences, 13*, 1154. DOI: https://doi.org/10.1007/s12517-020-06154-4

Alvarez, D. G. & Olmedo, M. T. C. (2023). Analysing the inconsistencies of CORINE status layers (CLC) and layers of changes (CHA) (1990-2018) for a Spanish case study. *Annals of GIS, 29*(3), 369-386. DOI: https://doi.org/10.1080/19475683.2023.2166583

Baduna Koçyiğit M., Akay H. (2018). Estimation of potential flash flood risk in a basin using morphometric parameters: A case study of Akçay Basin. *Journal of the Faculty of Engineering and Architecture of Gazi University*, *33*(4), 1321-1332.

Beven, K. J. (2012). *Rainfall-Runoff modelling.* England: John Wiley and Sons.

Chadli, K., Kirat, M., Laadoua, A. & El-Harchaoui, N. (2016). Runoff modeling of Sebou watershed (Morocco) using SCS curve number method and geographic information system. *Modeling Earth Systems and Environment, 2*(158). DOI: https://doi.org/10.1007/s40808-016-0215-6

Cinar, M. (2023) Investigation of mechanical and physical features of cementitious jet grout applications for various soil types. *Buildings, 13*(11). DOI: https://doi.org/10.3390/buildings13112833.

Coordination of Information on the Environment [CORINE]. (2021, July 12). *CORINE Land Cover data website*. Retrieved from https://land.copernicus.eu/en/products/corine-land-cover/clc2018

Cosun, F., & Karabulut, M. (2009). Mean, minimum and Maximum temperature trends in kahramanmaras. *Turk Cografya Dergisi, 53*, 41-50. Retrieved on June 23, 2023 from https://dergipark.org.tr/en/download/article-file/198465

Cubuk, M. H., & Dis, M. O. (2022). Development of Watershed Morphological Maps for the SCS-CN Methodology: Case Study over Sisne Basin. *KSU Journal of Engineering Sciences, 25*(2), 57-70. DOI: https://doi.org/10.17780/ksujes.1073949

Daniel, E. B., Camp, J. V., LeBoeuf, E. J., Penrod, J. R., Dobbins, J. P. & Abkowitz, M. D. (2011). Watershed Modeling and its Applications: A State-of-the-Art Review. *The Open Hydrology Journal, 5*(1), 26-50. DOI: https://doi.org/10.2174/1874378101105010026

Das, S. & Paul, P. K. (2006). Selection of site for small hydel using GIS in the Himalayan region of India. *Journal of Spatial Hydrology, 6*(1), 18-28.

De Ridder, N. A., & Boonstra, J. (1994). Analysis of water balances. In H. P. Ritzema (Ed.), *Drainage principles and applications* (2nd, p. 601-633). Wageningen, NL: International Institute for Land Reclamation and Improvement/ILRI.

Dis, M. O. (2023) A new approach for completing missing data series in pan evaporation using multi-meteorologic phenomena. *Sustainability, 15*(21). DOI: https://doi.org/10.3390/su152115542.

Dizdar, Y. (1984). Determination of runoff curve number in small basins. *Republic of Türkiye Ministry of Agriculture and Forestry, General Directorate of Soilwater Publications*, No: 749.

Elagca, A. & Dis, M. O., (2022). Application of Arc-GIS, HEC-GeoHMS and HEC-HMS in a Holistic Sense for Estimation of Rainfall-Runoff Process: Case Study over Ballikaya Basin. *Acta Scientiarum - Technology, 44*(1). DOI: https://dx.doi.org/10.4025/actascitechnol.v44i1.58360

Enemark, T., Peeters, L. J. M., Mallants, D. & Batelaan, O. (2019). Hydrogeological conceptual model building and testing: A review. *Journal of Hydrology, 569*, 310–329. DOI: https://doi.org/10.1016/j.jhydrol.2018.12.007

European Soil Data Centre [ESDAC]. (2021). *3D Soil Hydraulic Database of Europe at 1 km and 250m resolution*. Retrieved on July 14, 2021 from https://esdac.jrc.ec.europa.eu/

European Space Agency [ESA]. (2015). *Sentinel-2 User Hand Book* (Issue1.2). Retrieved from https://sentinel.esa.int/documents/247904/685211/sentinel-2_user_handbook

Fohrer, N., Haverkamp, S. & Frede, H. G. (2005) Assessment of the effects of land use patterns on hydrologic landscape functions: development of sustainable land use concepts for low mountain range areas. *Hydrological Process, 19*(3), 659-672. DOI: https://doi.org/10.1002/hyp.5623

Gassman, P. W., Reyes, M. R., Green, C. H. & Arnold, J. G. (2007). The soil and water assessment tool: historical development, applications, and future research directions. *Transactions of the ASABE, 50*(4), 1211–1250. DOI: https://doi.org/10.13031/2013.23637

Geographic Information Systems [GIS]. (2021). *Digital Elevation Model data set website*. Retrieved on July 26, 2021 from https://earthexplorer.usgs.gov/

Jehanzaib, M., Ajmal, M., Achite, M. & Kim, T. W. (2022). Comprehensive review: Advancements in rainfall-runoff modelling for flood mitigation. *Climate, 10*(10). DOI: https://doi.org/10.3390/cli10100147

Jin, H., Liang, R., Wang, Y. & Tumula, P. (2015). Flood-runoff in semi-arid and sub-humid regions, a case study: a simulation of jianghe watershed in northern China. *Journal of Water, 7*(9), 5155-5172. DOI: https://doi.org/10.3390/w7095155

Júnior, S. F. A. X., Stosic, T., Stosic, B., Jale, J. S. & Xavier, É. F. M. (2018). A brief multifractal analysis of rainfall dynamics in Piracicaba, São Paulo, Brazil. *Acta Scientiarum. Technology, 40*(1). DOI: https://doi.org/10.4025/actascitechnol.v40i1.35116

Knebl, M. R., Yang, Z.L., Hutchison, K. & Maidment, D. R. (2005). Regional scale flood modeling using NEXRAD rainfall, GIS, and HEC-HMS/RAS: a case study for the San Antonio river basin summer 2002 storm event. *Journal of Environmental Management, 75*(4), 325-336. DOI: https://doi.org/10.1016/j.jenvman.2004.11.024

Meric, B. T. (2004). Water Resources Management and Turkey. *Journal of Geological Engineering, 28*(1), 27-38.

Mesta, B., Kargi, P. G., Tezyapar, I., Ayvaz, M. T., Goktas, R. K., Kentel, E, & Tezel, U. (2019). Determination of rainfall-runoff relationship in Yenicegoruce Basin with HEC-HMS hydrologic model. *Pamukkale University Journal of Engineering Sciences, 25*(8), 949-955. DOI: https://doi.org/10.5505/pajes.2019.75133

Mishra, S. K., & Singh, V. P. (1999). Another look at SCS-CN method. *Journal of Hydrologic Engineering, 4*(3), 257-264. DOI: https://doi.org/10.1061/(ASCE)1084-0699(1999)4:3(257)

Mishra, S. K., & Singh, V. P. (2003). Soil Conservation Service Curve Number (SCS-CN) methodology. *Water Science and Technology Library, 42*, 84-146. DOI: https://doi.org/10.1007/978-94-017-0147-1_2

Mockus, V., Werner, J., Woodward, D. E., Nielsen, R., Dobos, R., Hjelmfelt, A., & Hoeft, C. C. (2009). Part 630 Hydrology National Engineering Handbook: Chapter 7. Hydrologic soil groups, *US Department of Agriculture: Natural Resources Conservation Service*.

Nickman, A., Lyon, S. W., Jansson, P. E., & Olofsson, B. (2016). Simulating the impact of roads on hydrological responses: examples from Swedish terrain. *Hydrology Research Journal, 47*(4), 767-781. DOI: https://doi.org/10.2166/nh.2016.030

Onchevski, O., & Mihara, M. (2021). Rainwater Harvesting as a Mean for Water Conservation in Ovche Pole Region, Macedonia. *Environmental and Rural Development, 12*, 95-102. Retrieved From https://iserd.net/ijerd121/12-1-15.pdf [Access Date: 03.02.2024]

Ozdemir, H. (2007). Application of SCS CN rainfall-runoff modeling using GIS and remote sensing: A case study of Havran river basin (Balıkesir). *Turkish Journal of Geographical Sciences, 5*(2), 1-12. DOI: https://doi.org/10.2139/ssrn.3395852

Phiri, D., Simwanda, M., Salekin, S., Nyirenda, V. R., Murayama, Y., & Ranagalage M. (2020) Sentinel-2 Data for Land Cover/Use Mapping: A Review. *Remote Sensing, 12*(14). DOI: https://doi.org/10.3390/rs12142291

Ray, R. K. (2018). Limitation of automatic watershed delineation tools in coastal region. *Annals of GIS, 24*(4), 261-274. DOI: https://doi.org/10.1080/19475683.2018.1526212

Republic of Türkiye Ministry of Agriculture and Forestry [MAF]. (2021). *CORINE Project*. Retrieved on July 22, 2021 from https://corine.tarimorman.gov.tr/corineportal/

Rizeei, H. M., Pradhan, B., & Saharkhiz, M. A. (2018). Surface runoff prediction regarding LULC and climate dynamics using coupled LTM, optimized ARIMA, and GIS-based SCS-CN models in tropical region. *Arabian Journal of Geosciences, 11*(53), 1-16. DOI: https://doi.org/10.1007/s12517-018-3397-6

Scharffenberg, W. A., & Fleming, M. J. (2010). *Hydrologic Modeling System HEC-HMS - User's Manual Version 3.5*. Davis, CA: US Army Corps of Engineers, Hydrological Engineering Center. Retrieved from https://www.hec.usace.army.mil/software/hec-hms/documentation/HEC-HMS_Users_Manual_3.5.pdf

Soil Conservation Service [SCS]. (1986). *Urban hydrology for small watersheds* (Technical Release 55). Washington DC: Natural Resources Conservation Service, United States Department of Agriculture.

Solomon, S., Qin, D., Manning, M., Chen, Z., Marquis, M., Averyt, K. B., ... Miller, H. L. (2013). *IPCC Climate Change 2013: The Physical Science Basis. Contribution of Working Group I to the Fifth Assessment Report of the Intergovernmental Panel on Climate Change*. Cambridge, UK: Cambridge University Press.

Stonestorm, D. A., Scanlon, B. R., & Zhang, L. (2009). Introduction to Special Section on Impacts of Land Use Change on Water Resources. *Water Resources Research, 45*(7). DOI: https://doi.org/10.1029/2009WR007937

Strager, M. P., Fletcher, J. J., Strager, J. M., Yuill, C. B., Eli, R. N., Petty J. T., & Lamont S. J. (2010). Watershed analysis with GIS: The Watershed characterization and modeling system software application. *Computers and Geosciences, 36*(7). 970-976. DOI: https://doi.org/10.1016/j.cageo.2010.01.003

Su Yönetimi Genel Müdürlüğü [SYGM]. (2018). *Flood Management* (Report by Republic of Turkey Ministry of Agriculture and Forestry - General Directorate of Water Management). Ankara, Turkey.

Wang, J., Yang, H., Li, L., Gourley, J. J., Khan, S. I., Yilmaz, K. K., Adler, R. F., ... Okello, L. (2011) The coupled routing and excess storage (CREST) distributed hydrological model. *Hydrological Sciences Journal, 56*(1), 84–98. DOI: https://doi.org/10.1080/02626667.2010.543087

Zhu, S., Wei, J., Zhang, H., Xu, Y., & Qin, H. (2023). Spatiotemporal deep learning rainfall-runoff forecasting combined with remote sensing precipitation products in large scale basins. *Journal of Hydrology, 616*. DOI: https://doi.org/10.1016/j.jhydrol.2022.128727

Zope, P. E., Eldho, T. I., & Jothiprakash, V. (2016). Impact of Land Use-Land Cover Change and Urbanization on Flooding: A Case study of Oshiwara River Basin in Mumbai, India. *Catena, 145*, 142-154. DOI: https://doi.org/10.1016/j.catena.2016.06.009